Comparison between α and proton sequential emission in $^{16}O(132\ MeV)+^{58}Ni$ deep inelastic collisions

R. Barná, D. De Pasquale, A. Italiano, A. Trifiró, and M. Trimarchi
Istituto Nazionale di Fisica Nucleare, Gruppo Collegato di Messina–Messina, Dipartimento di Fisica dell'Università–Messina, Salita Sperone 31, Vill. S. Agata 98166 Messina, Italy

V. Rauch, C. Beck, T. Bellot, C. Bhattacharya,* D. Disdier,† R. M. Freeman, F. Haas, R. Nouicer,‡ P. Papka, M. Rousseau,§ and O. Stezowski‖
Institut de Recherches Subatomiques, UMR7500, IN2P3/CNRS–Université Louis Pasteur Strasbourg, 23, rue du Loess, BP 28, F-67037 Strasbourg Cedex 2, France

A. Strazzeri
Dipartimento di Fisica dell'Università–Catania, Istituto Nazionale di Fisica Nucleare, Sezione di Catania–Catania, Corso Italia 57, 95129 Catania, Italy

(Received 13 March 2002; published 27 November 2002)

The $^{16}O+^{58}Ni$ deep-inelastic collision has been investigated at $E_{lab}(^{16}O)=132$ MeV by using coincident charged particle techniques. Exclusive data of the projectilelike fragments (C, N, and O) and their associated light charged particles (protons and α particles) were collected in coincidence. The experiment has been performed at the IReS Strasbourg VIVITRON Tandem facility by using the ICARE charged particle multidetector array. The measured velocity diagrams and in-plane angular correlations have been analyzed by a semiclassical model that combines equilibrium and nonequilibrium processes of a deep-inelastic scattering reaction. Following the hypothesis of a sequential process, this closed-form theoretical approach is applied to the measured [(C,N,O)-p] and [(C,N,O)-α] differential multiplicities. Estimates on polarization phenomena and on ''decay times'' are used to provide information about deep-inelastic scattering in $^{16}O+^{58}Ni$ at 8.25 MeV/nucleon.

DOI: 10.1103/PhysRevC.66.054607 PACS number(s): 25.70.Gh, 25.70.Jj, 25.70.Mn, 24.60.Dr

I. INTRODUCTION

The study of dinuclear systems formed in peripheral heavy-ion reactions as well as in deep-inelastic (DI) collisions at low bombarding energies not exceeding 10 MeV/nucleon [1] is still an interesting domain of research since the subsequent decay of these dinuclear objects by light-particle sequential emission is still not well understood. The light particle emission in DI collisions is a very powerful tool to investigate the various mechanims leading to the strong energy dissipation typical of this kind of reaction mechanisms [2–12]. DI collisions involve a large transfer of angular momentum from the entrance channel to the intrinsic spins of the projectilelike and targetlike reaction products. The amount of the angular momentum transferred, and its alignment, can be studied by measuring the angular distributions of the decay products of the excited targetlike fragments (TLF's) with respect to their recoil directions. Several studies of sequential processes [2,3,5,7–9] have revealed that the measured in-plane angular correlations are sharply forward peaked, and not symmetric with respect either to the direction of the projectilelike fragments (PLF's), or to the beam axis, with marked differences between distributions for positive and negative angles [7–9]. Despite of known sequential decay modes of DI fragments, clear experimental evidences were found for the occurence of an additional fast nonequilibrium emission of α particles in the $^{16}O+^{58}Ni$ reaction between 6 and 9 MeV/nucleon [2,5,7,8]. This fast α-decay mode implies that the reaction time has to be small compared to the rotational period of the intermediate dinuclear system. In order to describe this experimental behavior we have developed in a recent publication [13] a semiclassical approach [14–19], which combines both the fast nonequilibrium (NE) component and the slower evaporative contribution [equilibrium (E) component] of the sequential particle emission in peripheral heavy-ion collisions in a simple way. This approach was recently applied [13] to measured angular correlations between α particles and PLF's arising from the $^{16}O(96\ MeV)+^{58}Ni$ [2,5,7,8] and $^{16}O(133\ MeV)+^{48}Ti$ [13] DI collisions. Here we report on the analysis of the α and proton preequilibrium emission in the $^{16}O+^{58}Ni$ reaction at $E_{lab}=132$ MeV. The experiment has been performed at the VIVITRON Tandem facility with the ICARE charged particle multidetector array [20–22]. The angular correlations of protons have been measured for the first time for the $^{16}O+^{58}Ni$ reaction. A comparison between the two kinds of emission (NE and evaporative components) for both α particles and protons is made to give further information on the reaction mechanism: for example polariza-

*Permanent address: VECC, 1/AF Bidhan Nagar, Kolkata 64, India.

†Deceased.

‡Present address: Department of Physics, University of Illinois at Chicago, Chicago, Illinois 60607-7059.

§Present address: University of Surrey, Guildford GU2 7XH, United Kingdom.

‖Permanent address: IPN Lyon, F-69622 Villeurbanne, France.

tion effects and estimates of ''decay times.''

The paper is organized in the following way. After a short description of the experimental techniques, the experimental results are presented in Sec. II (part of the work presented here in detail has already been briefly reported elsewhere [23]). In Sec. III a description of the semiclassical model used to analyze the experimental data is first given, and then the application of the approach is carried on with a comparison between (C,N,O)-α and (C,N,O)-p angular correlations. A summary and concluding remarks are finally given in Sec. IV.

II. EXPERIMENTAL TECHNIQUES AND RESULTS

In the present study, we have considered the α particles associated with the C, N, and O PLF's which are emitted in the reaction plane by the Zn, Cu, and Ni TLF's during the sequential reaction

$$^{16}\mathrm{O}+{}^{58}\mathrm{Ni}\rightarrow(\mathrm{C,N,O})+(\mathrm{Zn^*,Cu^*,Ni^*})+Q_2$$
$$\rightarrow(\mathrm{C,N,O})+(\mathrm{Ni,Co,Fe})+\alpha+Q_3.$$

Similarly, we have measured the *in-plane* angular correlations of the protons associated with the C, N, and O PLF's which are emitted by the Zn, Cu, and Ni PLF's during the sequential reaction

$$^{16}\mathrm{O}+{}^{58}\mathrm{Ni}\rightarrow(\mathrm{C,N,O})+(\mathrm{Zn^*,Cu^*,Ni^*})+Q_2$$
$$\rightarrow(\mathrm{C,N,O})+(\mathrm{Cu,Ni,Co})+p+Q_3.$$

A. Experimental setup

The experiment has been performed at the IReS Strasbourg VIVITRON Tandem facility using a 132 MeV ^{16}O beam which was incident on an isotopically enriched ^{58}Ni (500 μg/cm^2 thick) target mounted in the ICARE scattering chamber [20–22]. The main purpose of this work was to investigate the *in-plane* angular correlations between the C, N, and O PLF's and the light charged particles (LCP's). We have measured both the [(C,N,O)-α] and [(C,N,O)-p] differential multiplicities, arising from the ^{16}O(132 MeV) + ^{58}Ni DI collision.

Both the heavy ions ($A\geqslant 6$) and their associated LCP's (p, d, t, and α particles) were detected using the ICARE charged particle multidetector array [20–22] which consists of 48 telescopes in coincidence. The strongly energy-damped PLF's (C, N, O) ions were detected in ten gas-silicon hybrid telescopes (IC), each composed of a 4.8 cm thick ionization chamber, with a thin Mylar entrance window, followed by a 750 μm thick Si(SB) detector. The IC telescopes allow a good resolution in emission angle, kinetic energy, and Z of the detected particle. Three of the IC's were placed at an angle of $\vartheta_{\mathrm{lab}}=30°$ with respect to the beam direction, well above the grazing angle ($\vartheta_{\mathrm{grazing}}=20°$ for the studied system). The reaction plane is defined by the beam axis and the direction flight of the detected PLF's, i.e., the IC location.

The present investigation of the LCP angular correlations has been restricted to measurements in the reaction plane, with 33 telescopes (of the total number of 48 telescopes) of ICARE put in the reaction chamber on two rings intersecting each other along the beam direction. Two IC telescopes were mounted on the first ring, at $\vartheta_{\mathrm{lab}}=+30°$ and $\vartheta_{\mathrm{lab}}=-30°$ with respect to the beam axis, while a third one was mounted on the second ring, at $\vartheta_{\mathrm{lab}}=+30°$. The remaining seven IC telescopes were mounted (on the first ring) at backward angles ($\vartheta\geqslant 120°$), having a low-energy threshold needed to detect very low energy particles emitted in the backward angle region. The IC's were filled with isobutane at a pressure of 60 Torr for the backward angle telescopes and 120 Torr for the forward angle detectors, thus allowing for the simultaneous measurement of both light and heavy fragments.

The in-plane detection of coincident LCP's has been done using 16 two-element telescopes [40 μm Si, 2 cm CsI(Tl)], with high-energy thresholds, mounted, on the first ring, in the $\vartheta_{\mathrm{lab}}=40°-120°$ angular range. seven three-element telescopes [40 μm Si, 300 μm Si, and 2 cm CsI(Tl)] were mounted on both rings, between $\vartheta_{\mathrm{lab}}=10°$ and $\vartheta_{\mathrm{lab}}=35°$, where the kinetic energy of the light particles has its maximum. By adopting this geometry, collection of the coincidences between the PLF telescopes and each LCP telescope for both rings allowed the investigation of 54 angles on the whole in-plane angular range. The CsI(Tl) scintillators were coupled to photodiode readouts. To lower the detection threshold for the LCP's and to provide a mass identification, time-of-flight measurements were also made for the slow LCP stopped in the ΔE detectors.

B. Experimental procedures and data analysis

The energy calibrations of the different telescopes of the ICARE multidetector array were carried out by using ^{228}Th and ^{241}Am radioactive α-particle sources in the 5–9 MeV energy range, a precision pulser, and elastic scatterings of 132 MeV ^{16}O from ^{197}Au, ^{58}Ni, and ^{12}C targets in a standard manner. In addition, the $^{12}\mathrm{C}(^{16}\mathrm{O},\alpha)^{24}\mathrm{Mg}^*$ reaction at $E_{\mathrm{lab}}=53$ MeV [22] has been used to provide known energies of α particles feeding the ^{24}Mg excited states, thus allowing the α calibration of the LCP telescopes. The proton calibration has been carried out using scattered protons from formvar targets bombarded in reversed kinematics reactions with the two ^{16}O beams.

A typical example of PLF's charge identification which can be achieved from the E-ΔE two-dimensional spectrum registered at $\vartheta_{\mathrm{lab}}=-30°$ is displayed [24] in Fig. 1(a). This plot shows how clearly the identification of the fragments can be achieved, due to the excellent charge resolution by the IC's allowing us to distinguish among them. Figure. 1(b) displays a typical bidimensional E-ΔE spectrum for a LCP telescope located at $\vartheta_{\mathrm{lab}}=+30°$. The charge and mass identifications for p, d, and t as well as for ^{3}He and α particles have been clearly achieved for all LCP telescopes. To lower the detection threshold for the LCP's and to provide a mass identification, time-of-flight measurements were also made for the slow LCP stopped in the ΔE detectors. More details on the experimental setup of ICARE and on the experimental procedures can be found in Refs. [22,25,26].

C. Experimental results

The velocity contour maps of the LCP Galilean invariant differential cross sections $(d^2\sigma/d\Omega dE)p^{-1}c^{-1}$ as a function

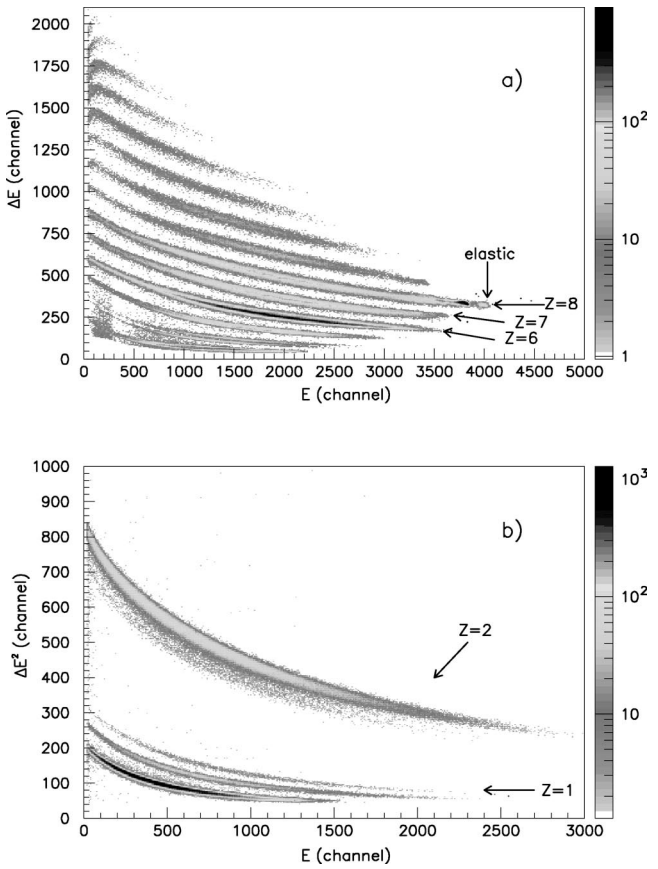

FIG. 1. Examples of charge identification from two typical E-ΔE bidimensional spectra measured for the $^{16}O+^{58}Ni$ reaction at $E_{lab}=132$ MeV with a IC telescope located at $\vartheta_{lab}=-30°$ (a), and a LCP telescope located at $\vartheta_{lab}=+30°$ (b).

of the LCP velocity provides an overall picture of the reaction pattern. Figure 2 shows such a velocity diagram of invariant cross section in the $(V_{\parallel},V_{\perp})$ plane for α particles measured in coincidence with C, N, and O fragments emitted at 30°. The symbols $V_{\parallel}$ and $V_{\perp}$ denote laboratory velocity components parallel and perpendicular to the beam, respectively. Figure 3 shows the analogous velocity diagram for protons.

In Figs. 2 and 3 the arrows indicate, for the $^{16}O+^{58}Ni$, the (average) recoil velocity vectors corresponding to the PLF and TLF emission sources, respectively. The ellipsoidal curves and the circles centered at the tips of these arrows mark the most probable velocities of the α particles and protons sequentially emitted from the fully accelerated binary fragments. It should be noticed that the appearance of an ellipse for α emission from the detected PLF's is due to the narrow velocity distribution of the primary fragment and the recoil imparted to the secondary fragment when the primary fragment decays. The radii of the circles associated with the TLF emission sources have been calculated by assuming the respective Coulomb barriers of α-TLF and p-TLF. The ellipsoidal curves have been calculated by fixing the PLF excitation energies to their most probable values, i.e., 10, 6, and 7 MeV for O*, F*, and Ne* fragments, respectively [21,27,28]. These calculated ellipsoidal curves display the occurrence of the two kinematical solutions of the α-emitting TLF's. Whereas the agreement with data appears to be satisfactory, it clearly shows an excess of yields at higher velocities indicative of the occurence of significant NE components.

The velocity diagrams of Figs. 2 and 3 show the complexity of separating the different emission sources whose contributions are mixed in the forward hemisphere, where the NE α emission is known to compete significantly in the angular correlations. In order to discriminate reactions with light target contaminations (mainly C and much less O), the carbon target measurements have been very carefully analyzed for all α detection angles as shown in Figs. 2 and 3. The comparison of the velocity diagrams for the ^{58}Ni and ^{12}C targets allow to distinguish a significant α component due to the C build-up contamination of the ^{58}Ni target. The amount of carbon impurity in the ^{58}Ni target has been estimated to be of approximately 10 $\mu g/cm^2$. This component is essentially present in the forward-angle region. In order to well identify the E and NE sequential components, all other processes contributing to the α and p emissions, e.g., the α particles arising from the C build-up contamination and the break-up events, have to be eliminated. The following substraction procedure has been used. First, and from the carbon target measurements, the DI α yields were derived by substracting the C build-up yields in each of the α energy spectra of all the 54 detection angles. Thereafter, the elastic and inelastic PLF breakup yields, which contribute more around the PLF emission direction, could be removed reasonably well by an extrapolation analysis of the α energy versus PLF energy correlations. This method allows us to evaluate the low-energy contribution starting from the high-energy one. It can be shown from the the velocity diagrams of Fig. 2 that the observed cross section for the high-energy contribution decreases monotonically with increasing α angle. This dependence is due to the angular variation of the inclusive PLF cross section, while the sequential emission is isotropic in the reference frame of the recoiling system.

Details on the procedure followed can be found in Refs. [21,27,28]. The analyzed in-plane angular correlation data are transformed to the rest frame of the recoiling TLF (Zn, Cu, and Ni, respectively).

Figure 4 shows the experimental data of the cross sections for (C-α), (N-α), and (O-α) coincidences together with the theoretical curves described in the following section, plotted vs the in-plane α angle measured with respect to the beam direction, respectively. Since we have adopted as a ''natural'' reference frame the ''recoil center of mass'' system [19], the ϕ_{α} (and, next, ϕ_p) angles undergo such a transformation. This is the reason why the ϕ values that are indicated by the arrows in Figs. 4 and 5 are not the same as for the detector angles of the experimental setup. The forward-angle region appears to be dominated by the preequilibrium component, which strongly depends on the mechanism of the first reaction step, while at backward angles only the E emission is present, and this component is almost isotropic for all the three coincident exit channels. The in-plane differential multiplicities of (C-p), (N-p), and (O-p) vs the φ_p angle are shown in Fig. 5. The same y scale adopted in both Figs. 4

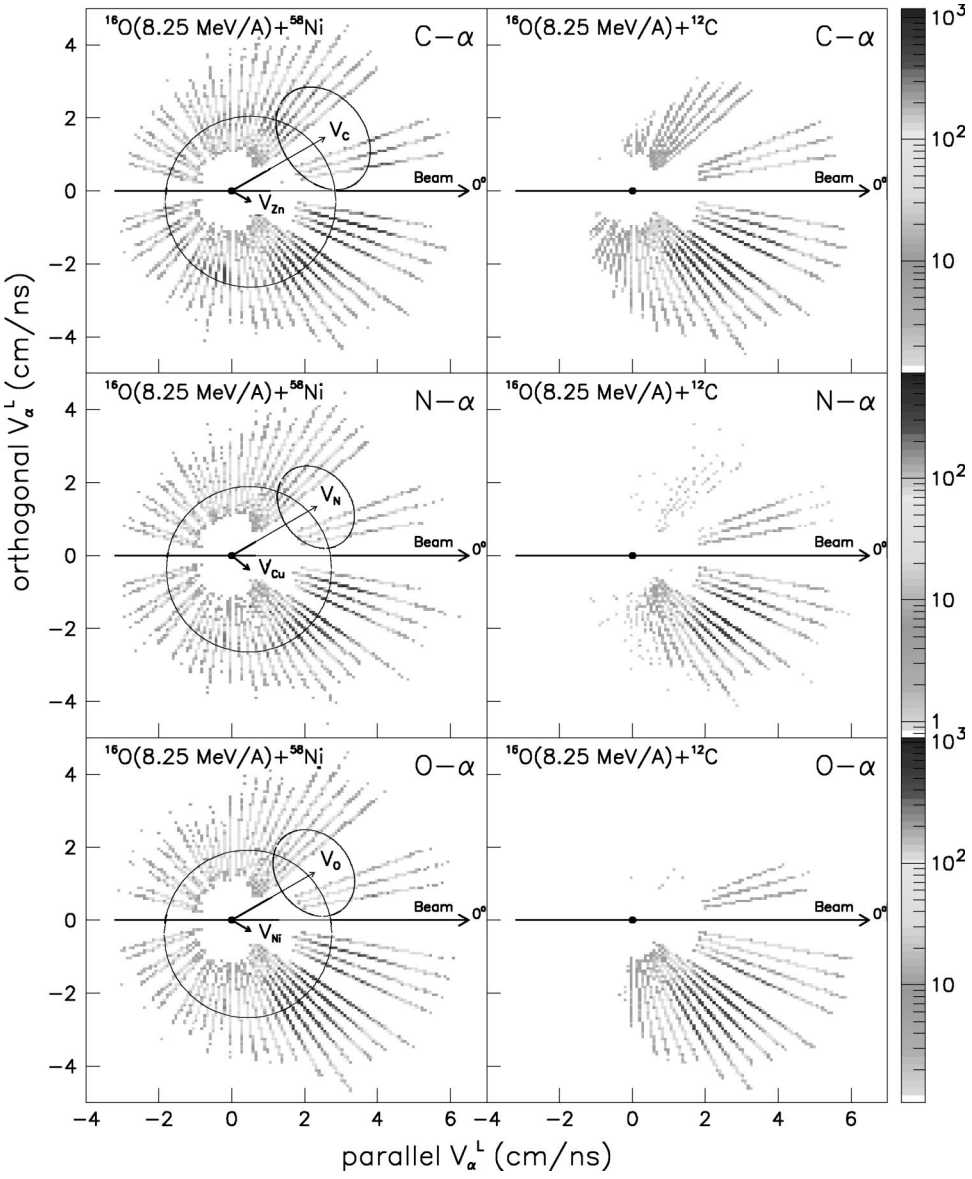

FIG. 2. Exclusive Galilean invariant cross section $(d^2\sigma/d\Omega dE)p^{-1}c^{-1}$ of α particles in coincidence with C,N,O fragments identified in a IC located at $\Theta_{\rm lab}^{\rm C}=30°$, as plotted in the $(V_\parallel,V_\perp)$ plane for the ^{16}O+^{58}Ni (left side) and ^{16}O+^{12}C (right side) reactions at $E_{\rm lab}=132$ MeV.

and 5 allows a direct comparison of the differential multiplicities for the α and proton emissions, respectively.

III. SEMICLASSICAL APPROACH TO PARTICLE-PARTICLE ANGULAR CORRELATION

A. Theoretical background

The theoretical background of the semiclassical model of Refs. [18,19] has already been described in a previous publication [13]. Let us recall some of the fundamental formulas for a better understanding of the physical meaning of the deduced quantities which will be discussed later in the following section as well as in the conclusions which will be drawn at the end of the paper.

The main aim of the theoretical approach is to outline a closed-form expression for the b-c multiplicity of a three-body sequential process such as $A(a,b)B(c)C$ showing that a significant NE component in the particle emission is present even in the case of a sequential process. We also show how useful conclusions on the mechanism of a peripheral collision $A(a,b)B$ can be drawn from the investigation of the b-c angular correlation pattern around the forward angles.

We start by considering [17–19] a three-body sequential process such as $A(a,b)B(c)C$ that assumes it proceeds through a given continuum state $(\epsilon_B^\star, J_B\pi_B)$ in the nucleus B to a narrow definite state $(\epsilon_C^\star, J_C\pi_C)$ in the final nucleus C.

In the following, $\epsilon_X^\star$ indicates the excitation energy of the state of definite spin J_X and parity π_X in the nucleus X and m_X the z component of $\vec{J}_X$. The pair (xX) has relative radial coordinate $\vec{r}_x$, momentum $\vec{k}_x$, velocity $\vec{v}_x$, and energy ϵ_x. The spherical polar angles (ϑ_b,φ_b) of $\vec{k}_b$ are defined in the $(A+a)$ center-of-mass (c.m.) system, while $\vec{k}_c$ has polar angles (ϑ,φ) defined in the recoil center-of-mass (r.c.m.) system (rest frame of the nucleus B) and described in a xyz frame with the x axis and z axis parallel to the x axis and z axis of the c.m. frame [14,16].

In order for the $A(a,b)B(c)C$ reaction to be a sequential process, we require that the $\epsilon_B^\star$ excitation energy of the in-

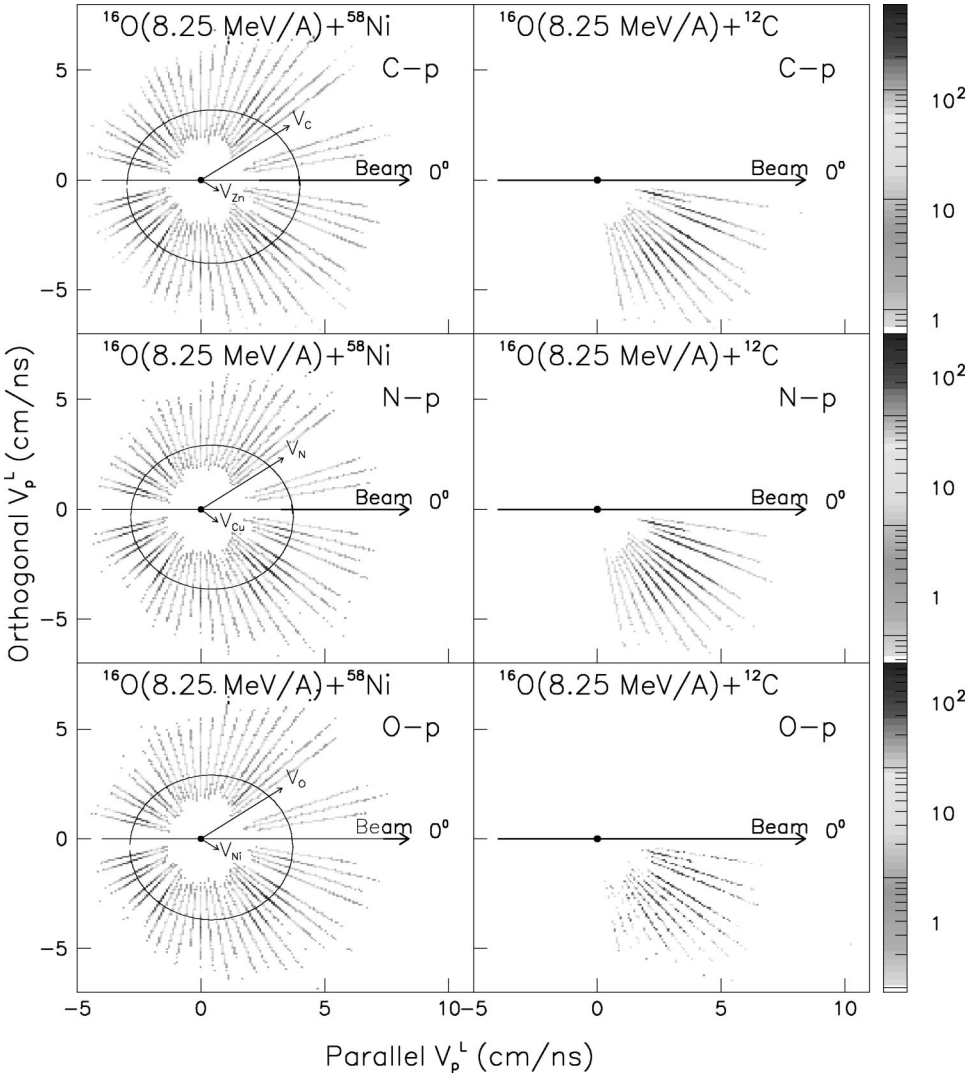

FIG. 3. Exclusive Galilean invariant cross section $(d^2\sigma/d\Omega dE)p^{-1}c^{-1}$ of protons in coincidence with C, N, O fragments identified in a IC located at $\Theta_{lab}^{C}=30°$, as plotted in the $(V_{\parallel},V_{\perp})$ plane for the ^{16}O+^{58}Ni and ^{16}O+^{12}C reactions at $E_{\rm lab}=132$ MeV.

termediate system B formed in the first step of the three-body reaction be independent of the particle c emission angle and assume, moreover, that in the $B\rightarrow c+C$ decay the nuclear interaction between b and B can be neglected. For the sake of simplicity, we suppose that the nuclei $A,a,b,$ and c have spin zero and b and c are in the ground state [17].

The average value of the b-c angular correlation over the energy interval Δ centered at energy $\epsilon_B^{\star}$, can be obtained by splitting the $\mathcal{S}$ matrix into an E and a NE term as [29]

$$\mathcal{S}=\mathcal{S}^{E}+\mathcal{S}^{\rm NE} \tag{1a}$$

with

$$\mathcal{S}^{E}=\mathcal{S}-\langle\mathcal{S}\rangle, \tag{1b}$$

$$\mathcal{S}^{\rm NE}=\langle\mathcal{S}\rangle. \tag{1c}$$

Moreover we suppose the phase of $\mathcal{S}^{E}$ and $\mathcal{S}^{\rm NE}$ to be uncorrelated (so that their cross terms average out to zero) and we make the statistical assumption that in the energy interval Δ around $\epsilon_B^{\star}$ there are many levels contributing to the $B\rightarrow c+C$ decay and that their widths and energies are randomly distributed, so that interference terms generally vanish [30,31].

We also assume that the amplitude $\mathcal{S}^{\rm NE}$ [see Eq. (1c)] is a very smoothly varying function of the excitation energy $\epsilon_C^{\star}$ within a $\Delta'(\sim\Delta)$ region. By considering ω_b and ω as the solid angles of the corresponding PLF and LCP detectors, respectively (as defined in Fig. 1 of Ref. [19]), we can express the energy averaged b-c angular correlation as the sum

$$\left\langle\frac{d^2\sigma}{d\omega_b d\omega}\right\rangle=\left(\frac{d^2\sigma}{d\omega_b d\omega}\right)^{E}+\left(\frac{d^2\sigma}{d\omega_b d\omega}\right)^{\rm NE} \tag{2}$$

with

$$\left(\frac{d^2\sigma}{d\omega_b d\omega}\right)^{E}=\sum_{m_C}\sum_{lJ_C} w_l(J_C)\left(\frac{T_l}{G}\right)\left|\sum_{m_B} p_l(m_B,m_C;\omega_b,\omega)\right|^2 \tag{3}$$

$$\left(\frac{d^2\sigma}{d\omega_b d\omega}\right)^{\rm NE}=\sum_{m_C}\left|\sum_{lJ_C}\langle\mathcal{S}_l\rangle\sum_{m_B} p_l(m_B,m_C;\omega_b,\omega)\right|^2, \tag{4}$$

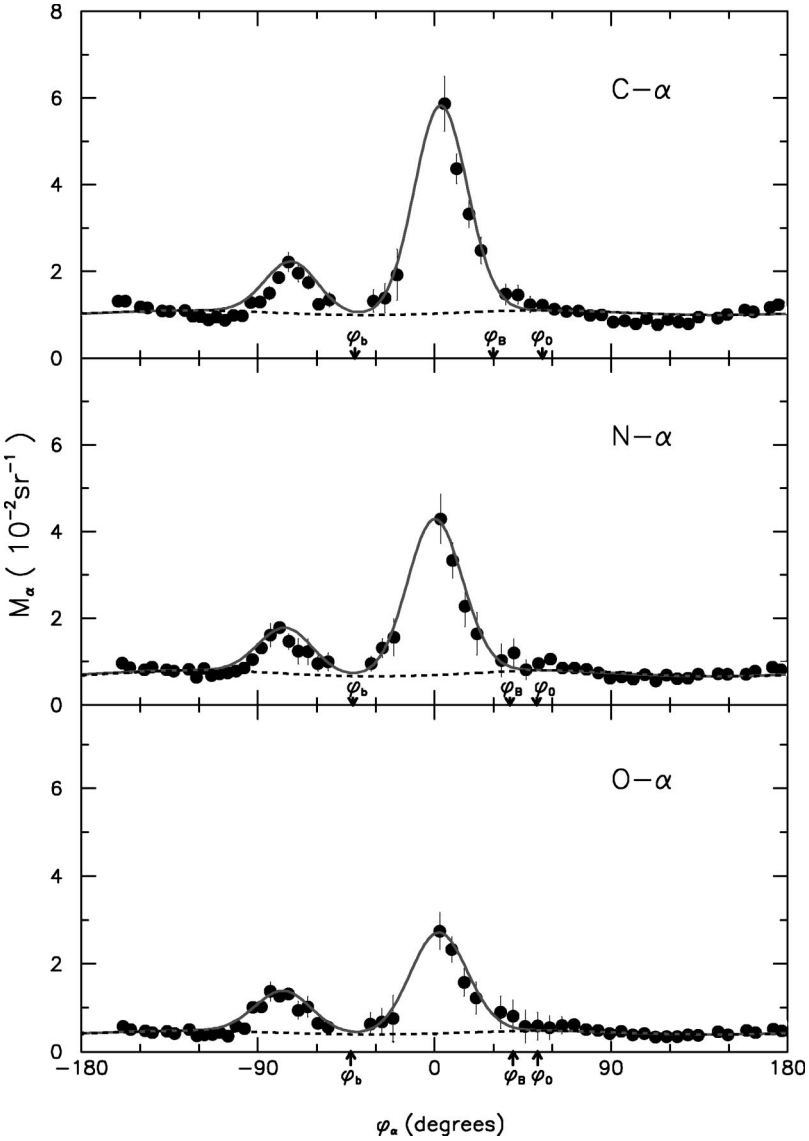

FIG. 4. Best fit of the in-plane C-α, N-α, and O-α angular correlation data, for the $^{16}O+^{58}Ni$ reaction at $E_{lab}=132$ MeV. The differential multiplicities, in 10^{-2} sr^{-1} units, are plotted in the recoil center of mass system vs the in-plane α angle. The arrows indicate in the recoil center of mass system the directions of the PLF (b) and the TLF (B) in the rest frame of the recoiling TLF with respect to the beam axis (see text). The solid curves represent the total ($E+$NE) multiplicities, while the dashed curves represent the equilibrium E component.

where

$$p_l(m_B,m_C;\omega_b,\omega)\equiv(-)^l F_{ba}(m_B,\omega_b)\times\langle lJ_C,m_B - m_C,m_C|J_B m_B\rangle Y_l^{m_B-m_C}(\omega). \quad (5)$$

In these expressions the decay amplitude $F_{ba}(m_B,\omega_b)$ [and hence the differential cross section for the reaction $A(a,b)B$] is a slowly varying function of the excitation energy which is defined in the basic equations quoted in Refs. [18,19] (see Eq. (3) of Ref. [18]). $F_{ba}(m_B,\omega_b)$ is related, through the proper Jacobian, to the amplitude f_{ba} which determines the population of the substate characterized by (J_B,m_B), in the nucleus B, prepared by detecting the b particle [19].

The quantity $w_l(J_C)$ which is related to the relative density of available states $(\epsilon_C^\star,J_C\pi_C)$ in the nucleus C, takes into account the probability of orbital angular momentum l transferred in the $B\rightarrow c+C$ decay into the $(B;J_B\epsilon_B^\star)\rightarrow(cC;lJ_C\epsilon_C^\star)$ decay, and assumes the parametrization $\langle|\mathcal{S}^E|^2\rangle=T_l/G$, where T_l is the optical-model transmission coefficient, G representing all decay modes energetically allowed for the $B\rightarrow c+C$ decay [30,31]. In particular, we are interested in the study of the following kinds of reactions:

$$a+A\rightarrow b+B\rightarrow b+\alpha+C$$

or

$$a+A\rightarrow b+B\rightarrow b+p+C.$$

The time-dependent scattering theory [32] allows us to assume that the quantity $(d^2\sigma)^{NE}$ can be associated with a situation in which the dissociation of B into c and C is a fast process occurring in time scales by many orders of magnitude shorter than the typical time corresponding to the equilibrium decay process, described by $(d^2\sigma)^E$, whose long lifetime in some way produces a ''loss of memory'' of the formation of the B decaying nucleus [31]. This is why the angular symmetry of the c-emission from a statistical equili-

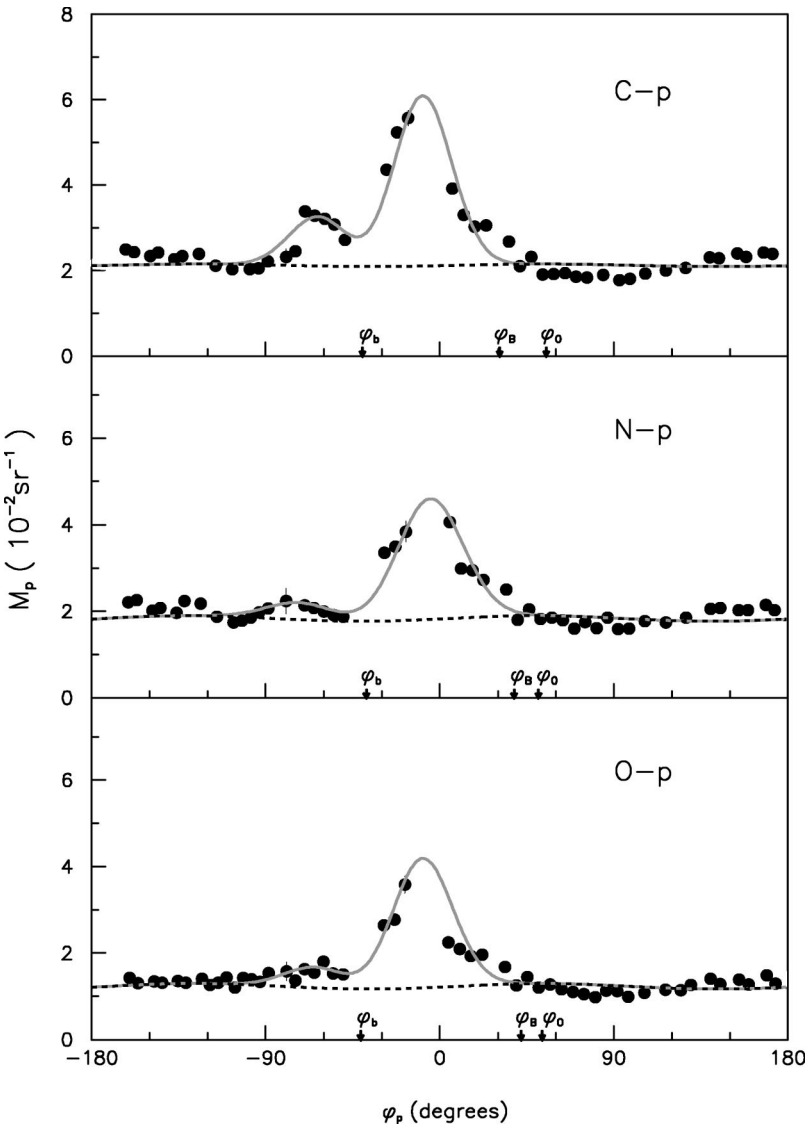

FIG. 5. Best fit of the in-plane C-p, N-p, and O-p angular correlation data, for the sequential process ^{16}O+^{58}Ni at $E_{\rm lab}$=132 MeV. The differential multiplicities, in 10^{-2} sr^{-1} units, are plotted in the recoil center of mass system vs the in-plane proton angle. The arrows indicate in the recoil center of mass system the directions of the PLF (b) and the TLF (B) in the rest frame of the recoiling TLF with respect to the beam axis (see text). The solid curves represent the total ($E+NE$) multiplicities, while the dashed curves represent the E component.

brated system described by the b-c angular correlation (3) cannot be used as evidence for any particular model of dynamical effect.

The memory of the first step of the sequential process $A(a,b)B(c)C$ is assumed to be retained during the subsequent "fast" $B\rightarrow c+C$ decay, so that the angular dependence of the c particles emerging from such a short-lived composite system can display a marked forward-backward asymmetry around the direction of the coincident projectile residue b or the beam axis. The study of the NE sequential component of the particle emission therefore becomes a powerful tool to probe the early stage of the peripheral collision in addition to a useful alternative technique to obtain nuclear structure or reaction mechanism information complementary to what is usually extracted by means of the angular distributions of the two-body reaction products [17].

Since the angular correlation method is mainly devoted to obtain information on the mechanism of the $A(a,b)B$ reaction and on the polarization effects of the B nucleus, it would be appropriate to adopt coordinate axes such that the z-axis is along $\vec{k}_b\times\vec{k}_a$ (perpendicular to the reaction plane) and the x axis along $\vec{k}_a$.

Information on the polarization effects of the residual nucleus B induced by the first step of the sequential process $A(a,b)B(c)C$, and left in general polarized in the reaction, can also be obtained through the φ dependence of the differential multiplicity for the second step [18,19].

A semiclassical expression for the b-c differential multiplicity has been treated and developed in Refs. [18,19] which accounts for many of the observed features of the sequential emission of the high as well as low energy particles from the fragments excited in a peripheral heavy-ion reaction. Without going into the details of the theoretical approach [18,19], we consider a semiclassical picture that assumes a coordinate rotation by means of the Euler angles $(\xi,\Lambda,0)$ to a more useful system described below. The rotation of axes defined by the Euler angles and the coordinate system chosen to describe the $B\rightarrow c+C$ decay can be visualized in Fig. 2 of Ref. [19].

Note that in reaction between heavy ions DI collisions are likely to produce nuclei having the intrinsic angular momentum predominantly oriented perpendicular to the reaction plane. The new quantization axis is oriented in the direction of $\vec{J}_B$ which is at an angle

$$\Lambda = -\cos^{-1}\left(\frac{m_B}{J_B}\right) \tag{6}$$

with respect to the normal z axis and lies in a plane perpendicular to the reaction plane and to the direction of a unit vector $\hat{k}_0$, close to the recoil direction of the decaying nucleus B [33], corresponding to an angle $\varphi_0=(\pi/2+\xi)$ with respect to the x axis. Consequently, the relative momentum $\vec{k}_c$ of the pair (cC) has polar angles (ϑ,φ) and (Θ,Φ) with respect to the space-fixed system and to the $(\hat{k}_0 \times \hat{J}_B, \hat{k}_0, \hat{J}_B)$-axes, respectively. The average value Λ_0 of the angle between the spin direction and the normal z-axis will be discussed more deeply in the theoretical analysis.

We introduce the variable $\mu=J_B$-J_C instead of J_C in the quantity w_l of Eq. (3), and we assume the following semiclassical replacement [34,35] in the well-known quantal treatment elaborated by Ericson and Strutinsky [34]:

$$w_l(\mu) \sim \exp(-\alpha l^2)\exp(\beta\mu), \tag{7}$$

where

$$\alpha \equiv (\mathcal{I}+MR^2)\hbar^2/2\mathcal{I}T_C MR^2,$$

$$\beta \equiv J_B\hbar^2/\mathcal{I}T_C$$

with M, R, and $\mathcal{I}$ the reduced mass, the radius, and the rigid-body moment of inertia of the pair (cC), respectively, and T_C the nuclear temperature corresponding to the excitation energy $\epsilon_C^\star$ in the C nucleus.

By using the *sharp cutoff* approximation for the coefficient transmission T_l and converting the summation over l to an integral, one obtains

$$[M(\vartheta,\varphi,\Lambda)]^E = C_E \exp(-\gamma\cos^2\Theta), \tag{8}$$

C_E being independent of ϑ and φ, while $\gamma \equiv \beta^2/4\alpha$ is the so-called anisotropy coefficient [35].

The "direct" sequential $B \to c+C$ decay described by $\langle \mathcal{S} \rangle$ [see Eq. (1)] is naturally attributed to a *prompt* emission of particles from peripheral regions of the nucleus B bearing in mind that in the classical limit the c particles while escaping from the rotating nucleus B gain additional velocity if emitted along the equatorial plane.

We estimate the NE b-c multiplicity by assuming that the emission of particles c in the equatorial plane with orbital angular momentum $\vec{l}$ parallel to $\vec{J}_B$ dominates and, we further assume that the peripheral nature of the NE decay process is consistent with the hypothesis that only an "l window," centered at an average value $l=l_0$, contributes. Therefore in the amplitude-phase representation the energy-averaged element $\langle \mathcal{S}_l \rangle$ becomes approximately near $l=l_0$:

$$\langle \mathcal{S}_l \rangle \sim \eta(l-l_0)\exp[i(l-l_0)\chi_0], \tag{9}$$

if we assume the Taylor expansion of the phase $\delta(l)$ to be linear about l_0 rather than of the second order with l [17], i.e., $\delta(l) \approx \delta(l_0)+(l-l_0)\chi_0$, where

$$\chi_0 \equiv \left(\frac{\partial\delta(l)}{\partial l}\right)_{l_0} \tag{10}$$

is the so-called quantal deflection function which somehow describes the "classical trajectory" of the particle c and the nucleus C in their mean field characterized by the phase shift δ [36]. By taking into account the relative amplitude h_0, which is associated with the negative polarization of the decaying residue B [19], and defined as the ratio

$$h_0 = |f_{ba}(-m_0,\omega_b)|^2/|f_{ba}(m_0,\omega_b)|^2,$$

where f_{ba} is linked to the F_{ba} amplitude by means of the proper Jacobian (see Ref. [19]), the NE differential multiplicity can be written as follows:

$$[M(\vartheta,\varphi,\Lambda)]^{\mathrm{NE}} \sim |Q^{(+)}(\Phi)|^2 + h_0|Q^{(-)}(\Phi)|^2, \tag{11}$$

where we have defined the "single source" amplitudes

$$Q^{(\pm)}(\Phi) \equiv \sum_l \eta(l-l_0)\exp[i(l-l_0)(\chi_0 \pm \Phi)].$$

Recalling the peripheral nature of the direct NE process, we can assume the amplitude $\eta(l-l_0)$ as a Gaussian distribution [37]

$$\eta(l-l_0) \sim \exp[-(l-l_0)^2/4\lambda^2],$$

and then following the approximations suggested in Refs. [18,19], Eq. (11) finally becomes

$$[M(\vartheta,\varphi,\Lambda)]^{\mathrm{NE}} = C_{\mathrm{NE}}\{\exp[-\lambda^2(\Phi+\chi_0)^2] + h_0\exp[-\lambda^2(\Phi-\chi_0)^2]\}. \tag{12}$$

The model parameter λ, which represents the width of the "l window," is of importance as it is related with the width of the peaks observed in the experimental angular correlations displayed in Figs. 4 and 5. It is interesting to note that C_{NE} contains all the nonessential constants independent of ϑ and φ.

For the sake of simplicity, the spin orientation is governed by a Gaussian distribution function $L(\Lambda)$ around the average value Λ_0, i.e., $L(\Lambda)=\exp[-(\Lambda\text{-}\Lambda_0)^2/\Omega^2]$. We have

$$M(\vartheta,\varphi) = [[M(\vartheta,\varphi)]^E + [M(\vartheta,\varphi)]^{\mathrm{NE}}] \tag{13}$$

with

$$M(\vartheta,\varphi)^E = \int d\Lambda L(\Lambda)(M(\vartheta,\varphi,\Lambda))^E / \int d\Lambda L(\Lambda), \tag{14}$$

$$M(\vartheta,\varphi)^{\mathrm{NE}} = \int d\Lambda L(\Lambda)(M(\vartheta,\varphi,\Lambda))^{\mathrm{NE}} / \int d\Lambda L(\Lambda), \tag{15}$$

where M^E and M^{NE} are given by Eqs. (8) and (12).

The NE in-plane b-c differential multiplicity corresponds to $\vartheta=\pi/2$, and is expected to exhibit a two-component

asymmetric patern (since in general the relative amplitude h_0 is non-null) about a direction close to the one of the detected ejectile $\xi=\varphi_0-\pi/2$ angle (see Fig. 2 of Ref. [19]). For example, in the simple case of complete alignment, the two components are peaked at the $\varphi_1=\xi-\chi_0$ and $\varphi_2=\xi+\chi_0$ angles, respectively. Moreover, if $\chi_0<\xi$ and $h_0<1$, the *b*-*c* coincidence events most probably appear on the same side of the beam axis with respect to the direction of the ''detected'' projectile residue. The in-plane coincidence cross sections around φ_1 and φ_2 correspond to the $A(a,b)B$ reaction process with opposite polarization of *B*. This may qualitatively be explained by assuming that only one type of ''semiclassical trajectory'' mainly contributes to the in-plane *b*-*c* angular correlation for either positive or negative angles with respect to the direction of the PLF *b* [36,39].

In the cases when the alignment is almost complete (as in the present data) with $\Lambda \ll 1$, one can obtain an estimate of the angle ξ, which is related to the direction ϕ_0 of the momentum transferred to the projectile-target interaction, and of the quantal deflection χ_0 by a simple inspection of the experimental in-plane angular correlation pattern around the ''peak angles'' φ_1 and φ_2, using the expressions

$$2\xi \simeq \varphi_2+\varphi_1, \tag{16}$$

$$2\chi_0 \simeq \varphi_2-\varphi_1. \tag{17}$$

Indeed here the deviation from left-right symmetry in a direction close to the one of the coincident projectile residue as well as the double forward-peaked shape in the angular correlation pattern does not necessarily imply that the light particles emerge from the contact zone between the two colliding nuclei (spatial localization). In a simple optical picture, we can interpret the sums appearing in Eq. (12) [see also Eq. (13)] as a beam of particles *c* emitted on the nuclear surface of the NE TLF from a ''*l* window'' centered about a mean value l_0 and extended over a narrow width $\Delta l \sim \lambda$ (*l* localization).

From the above rough picture we can find the time dependence of the NE $B \rightarrow c+C$ decay; for example the observed strongly forward peaked in-plane angular correlation can be seen as a signature of an emission of the *c* light particles in decay times shorter than the rotational period of the *B* nucleus, taken to be the time required for a hypothetical complete revolution of the $(c+C)$ composite system. Moreover, as already shown, a simple semiclassical picture allows us to link the χ_0 deflection angle to the τ_0 NE decay time, via the rotational frequency of the rotating nucleus $\omega_0 = \hbar l_0/\mathcal{I}$:

$$-\chi_0 = \omega_0 \tau_0 = \frac{\hbar l_0}{\mathcal{I}} \tau_0. \tag{18}$$

B. Theoretical analysis

The in-plane angular correlations plotted in Figs. 4 and 5 for α particles and protons, respectively, have been fitted (solid lines) by the semiclassical equations given before. The dashed and solid lines correspond to the equilibrium (*E*) and total ($E+\mathrm{NE}$) components, respectively.

Since the mean excitation energy of the emitting TLF is about 60 MeV, a value lying in the continuum region of the excitation spectrum, we can apply the above described theoretical approach to our nuclear system.

For both kinds of spectra C_E, γ, Λ, and Ω parameters have been fitted by the purely evaporative *E* formula (13) using the *backward* region data ($|\varphi_{\text{light-particle}}| \geqslant 100°$), where the experimental data arise primarily from the *E* component. γ and Λ_0 are not uniquely determined by this procedure, since a range of possibilities can likewise hold; ξ could also be deduced by the evaporative component, but this one is not so sensitive to its choice.

1. α emission in the $^{16}O+^{56}Ni$ reaction

In the case of α emission shown in Fig. 4, the values obtained for the average angle between the spin direction and the normal axis Λ_0 (6° for all the three coincidences) and for the the spin fluctuations Ω (13°) show that the polarization direction of the emitting nucleus is nearly orthogonal to the reaction plane. The fact that the TLF rotational axis lies very close to the *z* axis allows an estimate of the values of χ_0 by rewriting formulas (16),(17) as follows:

$$\varphi_1 = \xi-\chi_0 = \varphi_0-\frac{\pi}{2}-\chi_0, \tag{19}$$

$$\varphi_2 = \xi+\chi_0 = \varphi_0-\frac{\pi}{2}+\chi_0. \tag{20}$$

Correspondingly, the C_{NE}, λ, and h_0 parameters have been obtained by fitting the *forward* angular region ($|\varphi_{\text{light-particle}}| < 100°$) by means of the (complete) formula (13), after inserting the values of the above determined C_{NE}, γ, Λ_0, Ω, ξ, χ_0 parameters.

The parameter values for the three angular correlations are reported in Table I. By assuming $(C_{\mathrm{NE}};\gamma;\Lambda_0)$ as free parameters, the complete experimental in-plane angular correlations of the differential multiplicities (for α's and protons) have been fitted with the $(C_E;\gamma;\Lambda_0;\Omega;\xi;\chi_0)$ respective values previously determined, and thus the values for $(C_{\mathrm{NE}};\lambda;h_0)$ parameters have been deduced.

Comparing the values of the C_E parameter reported in Table I to the values deduced in Table I of Ref. [13] with the same analysis at $E_{\mathrm{lab}}=96$ MeV, one can observe that the *E* components are approximately identical. In contrast, the values of the C_{NE} parameter increase by almost a factor 4, indicating that NE α emission appears to follow an exponential increasing trend between 6 and 8.2 MeV/nucleon. However the target dependence (see Table II of Ref. [13] for the analysis of the data of the ^{48}Ti target at $E_{\mathrm{lab}}=132$ MeV for the comparison) of the NE component is very weak. These results confirm the systematics previously proposed by Ho *et al.* [7] (see Fig. 4 of Ref. [7]).

2. Proton emission in the $^{16}O+^{56}Ni$ reaction

The same theoretical approach has been applied to the analysis of the PLF-proton angular correlations. Figure 5

TABLE I. List of the parameters obtained in the analysis of the in-plane PLF-α angular correlations arising from the ^{16}O(132 MeV)+^{58}Ni reaction.

Coincidences (10^{-2} sr^{-1})	C_E [a]	γ [a]	Λ_0 [a]	Ω [a]	ξ [b]	χ_0 [b]
C-α	1.1±0.1	2.0±0.1	(6±4)°	(13±2)°	(−33∓2)°	(−41∓2)°
N-α	0.8±0.1	4.0±0.2	(6±4)°	(13±2)°	(−33∓2)°	(−41∓2)°
O-α	0.48±0.05	4.0±0.2	(6±4)°	(13±2)°	(−33∓2)°	(−41∓2)°

Coincidences (10^{-2} sr^{-1})	C_{NE} [a]	λ [a]	h_0 [a]	ϕ_R	ϕ_0 [b]
C-α	4.4±0.4	2.5±0.3	0.25±0.03	(30±3)°	(57±3)°
N-α	3.5±0.4	2.3±0.2	0.30±0.04	(38±3)°	(57±3)°
O-α	2.5±0.3	2.4±0.2	0.36±0.05	(40±3)°	(57±3)°

[a]The quantities obtained by fitting the experimental data by the evaporative formula (13).
[b]The quantities estimated from a simple inspection of the experimental angular correlation patterns by using the approximate expressions (19) and (20).

shows the calculations (solid lines for the NE component and dashed lines for the E component) of the in-plane angular correlations of the differential multiplicities of C-p, N-p, and O-p vs the φ_p angle. From Table II it can be seen that, whereas the NE components for protons are comparable to the that for α particles, the E components are larger by at least a factor 2.

From the analysis of the fit parameters reported in Tables I and II, one easily infers that the spin direction is almost perpendicular to the reaction plane, as was supposed in the theoretical approach. As a matter of fact, the small average value found for the angle between the spin direction and the normal axis ($\Lambda_0 \leqslant 10°$) confirms this hypothesis for all three coincidences. The NE component consists of two bumps; the higher one is associated with the positive polarization, the lower with the negative one. The width of the peaks is related to the model parameter λ which represents the width of the l window mainly contributing to the decay process; such a rather small value which does not exceed $3\hbar$ confirms that we are dealing with a peripheral process. The last parameter obtained by the fit is ξ, which is related to the direction ϕ_0 of the momentum transferred to the projectile-target interaction; in the case of hard spheres, this direction would correspond to the recoil direction of the TLF (ϕ_R). As one can deduce from Tables I and II, the difference between these angles decreases for decreasing projectile-target mass transfer.

In addition, one can obtain a rough estimate of the in-plane integrated sequential E and NE α emission for the processes considered here; in fact, in the case of $\vartheta = \pi/2$, we can get

$$\int_{-\pi}^{\pi} d\phi M(\phi) = M^E + M^{\mathrm{NE}} \tag{21}$$

with

TABLE II. List of the parameters obtained in the analysis of the in-plane PLF-proton angular correlations arising from the ^{16}O(132 MeV)+^{58}Ni reaction.

Coincidences (10^{-2} sr^{-1})	C_E [a]	γ [a]	Λ_0 [a]	Ω [a]	ξ [b]	χ_0 [b]
C-p	2.2±0.2	0.5±0.03	(6±4)°	(13±2)°	(−35∓2)°	(−28∓2)°
N-p	1.9±0.2	1.3±0.07	(6±4)°	(13±2)°	(−39∓2)°	(−35∓2)°
O-p	1.3±0.1	2.0±0.1	(6±4)°	(13±2)°	(−37∓2)°	(−29∓2)°

Coincidences (10^{-2} sr^{-1})	C_{NE} [a]	λ [a]	h_0 [a]	ϕ_R	ϕ_0 [b]
C-p	4.0±0.4	2.7±0.3	0.29±0.04	(31±3)°	(57±3)°
N-p	2.8±0.3	2.4±0.2	0.14±0.02	(38±3)°	(57±3)°
O-p	3.0±0.3	2.6±0.3	0.16±0.02	(43±3)°	(57±3)°

[a]The quantities obtained by fitting the experimental data by the evaporative formula (13).
[b]The quantities estimated from a simple inspection of the experimental angular correlation patterns by using the approximate expressions (19),(20).

TABLE III. Values of rough approximations of M^E and M^{NE} for the PLF-α and PLF-p angular correlations from the ^{16}O(132 MeV)+^{58}Ni reaction.

	PLF-α		PLF-proton	
Coincidences	M^E	M^{NE}	M^E	M^{NE}
C-(light-particle)	4.1	1.2	2.7	1.9
N-(light-particle)	2.8	1.1	4.3	1.3
O-(light-particle)	1.5	0.4	3.5	1.3

$$M^E \sim \pi C_E[1-\exp(-\gamma)], \tag{22}$$

$$M^{\mathrm{NE}} \sim C_{\mathrm{NE}}(1+h_0)/\lambda. \tag{23}$$

The values of $M^E + M^{\mathrm{NE}}$, estimated within 30%, are listed in Table III. Although NE processes comparatively contribute less at low bombarding energy, they cannot be neglected at increasing bombarding energies.

As usual in our treatment, we can define a positive alignment parameter on a quantization axis perpendicular to the reaction plane as (omitting the explicit indication of ω_b)

$$p_0 = |f_{ba}(m_0)|^2 \quad [|f_{ba}(m_0)|^2 + |f_{ba}(-m_0)|^2] = (1+h_0)^{-1},$$

whose values are reported in Table IV. For both α particles and protons the values of this parameter show a dominant positive polarization probability. Despite rather large uncertainties (with error bars larger than 10–15 % for both α particles and protons) the values of the polarization parameters for protons in coincidence with either O or N PLF's appear to be slightly greater than those obtained for the α emission.

According to the Wilczynski model of DI reactions [38], which attributes the energy dissipation to frictional forces arising in the projectile-target contact region, up and down polarizations can be related to positive and negative deflection functions, respectively. Then, the observed positive polarization can be explained by assuming [39] that only one kind of *semiclassical trajectory*, i.e., the *far-side* one, predominantly contributes to the NE component of the sequential emission.

An interesting feature of the reaction mechanism can be obtained by observing that [18,19] the half-angle between the two peaks χ_0 can be related to the lifetime of the emitting nucleus [5] according to Eq. (18), where $\mathcal{I}$ is calculated as

$$\mathcal{I} \approx \mathcal{I}_{\mathrm{rigid}} \approx 0.0137 A^{5/3} \hbar^2.$$

If we apply Eq. (18) to our reaction with $l_0 \simeq 4\hbar$ we obtain

TABLE IV. Values of p_0 parameters for the PLF-α and PLF-p angular correlations from the ^{16}O(132 MeV)+^{58}Ni reaction.

p_0 for coincidences	C	N	O
α	0.80	0.77	0.74
p	0.78	0.88	0.86

$$\tau_0 \simeq 5 \times 10^{-22} \text{ s for } \alpha \text{ particles},$$

$$\tau_0 \simeq 7 \times 10^{-22} \text{ s for protons}$$

as an estimate of the ''decay time'' after the formation of the B decaying nucleus. The results summarized in Table IV are consistent with the ''decay times'' deduced in Ref. [13] for the ^{16}O(96 MeV)+^{58}Ni and ^{16}O(133 MeV)+^{48}Ti reactions.

IV. SUMMARY AND CONCLUDING REMARKS

The differential multiplicities obtained for both the α particles and the protons have been measured for the DI collisions ^{16}O+^{58}Ni at 8.2 MeV/nucleon using the ICARE charged-particle multidetector array [20–22] for energy-damped events. A newly developed theoretical semiclassical approach [13] assuming the hypothesis of a two-step sequential mechanism that combines E and NE processes is successfully applied to analyze quantitatively the measured in-plane angular correlations between α particles and protons detected in coincidence with PLF's.

From this analysis, one infers that the angular interval between the average transferred momentum in the ^{58}Ni(^{16}O,b)B reaction and the recoil nucleus B direction increases with the transferred mass from ^{16}O nucleus to ^{58}Ni nucleus. Many of the observed features of the sequential E emission and NE emission are well reproduced for both the α particles and the protons by means of this simple semiclassical approach [13]. In particular, we have found for the first time that NE proton emission exists significantly in the DI processes of the ^{16}O+^{58}Ni reaction. Some information of the reaction mechanisms has been extracted, such as polarization phenomena (which appear to be slighltly more sensitive for proton emission than α emission) or estimates of ''decay times.'' By a comparison of the present analysis of the ^{16}O+^{58}Ni reaction to previous one [13] of the ^{16}O+^{48}Ti reaction, the target dependence of the NE α emission is found to be rather weak. The projectile dependence of both the NE α and proton emission still have to be investigated in a systematical manner. Therefore, this work may stimulate further experimental studies on different nuclear systems aimed at a deeper investigation of the time scales (lifetimes of the targetlike fragments and ''decay times'' of the formed dinuclear systems) involved in DI collisions.

ACKNOWLEDGMENTS

The authors wish to thank the staff of the VIVITRON for providing us with good ^{16}O stable beams, M.A. Saettel for preparing the targets, and J. Devin and C. Fuchs for the excellent support in carrying out these experiments. We wish also to thank L. Romano and K. Krishan for a careful reading of the manuscript.

[1] W.U. Schröder and J.R. Huizenga, in *Treatise on Heavy-Ion Science*, Vol. 2 of Nuclear Sciences, edited by D.A. Bromley, (Plenum, New York, 1994).
[2] H. Ho, R. Albrecht, W. Dünnweber, G. Graw, S.G. Staedmanm, J.P. Wurm, D. Disdier, V. Rauch, and, F. Scheibling, Z. Phys. A **283**, 235 (1977).
[3] H. Ho, P.L. Gonthier, M.N. Namboodiri, J.B. Natowitz, L. Adler, S. Simon, K. Hagel, R. Terry, and A. Khodai, Phys. Lett. **96B**, 51 (1980).
[4] T.C. Awes, G. Poggi, C.K. Gelbke, B.B. Back, B.G. Glagola, H. Breuer, and V.E. Viola, Jr., Phys. Rev. C **24**, 89 (1981).
[5] H. Ho, R. Albrecht, H. Damjantschitsch, F.J. Demond, W. Kühn, J. Slemmer, J.P. Wurm, D. Disdier, V. Rauch, F. Scheibling, and T. Dössing, Z. Phys. A **300**, 205 (1981).
[6] R.K. Bhowmik, E.C. Pollacco, J.B.A. England, G.C. Morrison, and N.E. Sanderson, Nucl. Phys. **A363**, 516 (1981).
[7] H. Ho, P.L. Gonthier, W. Kühn, A. Pfoh, L. Schad, R. Wolski, J.P. Wurm, J.C. Adloff, D. Disdier, A. Kamili, V. Rauch, G. Rudolf, F. Scheibling, and A. Strazzeri, Phys. Rev. C **27**, 584 (1983).
[8] A. Strazzeri, J.C. Adloff, D. Disdier, A. Kamili, V. Rauch, G. Rudolf, F. Scheibling, and V. D'Amico, Nuovo Cimento A **89**, 333 (1985).
[9] H. Ho, G.Y. Fan, P.L. Gonthier, W. Kühn, B. Lindl, A. Pfoh, L. Schad, R. Wolski, J.P. Wurm, J.C. Adloff, D. Disdier, V. Rauch, and F. Scheibling, Nucl. Phys. **A437**, 465 (1985).
[10] B. Lindl, A. Brucker, M. Bantel, H. Ho, R. Muffler, L. Schad, M.G. Trauth, and J.P. Wurm, Z. Phys. A **328**, 85 (1987).
[11] W. Terlau, M. Burgel, A. Budzanowski, H. Fuchs, H. Homeyer, G. Roschert, J. Uckert, and R. Vogel, Z. Phys. A **330**, 303 (1988).
[12] M.F. Vineyard, S.E. Atencio, J.F. Crum, G.P. Gilfoyle, B.G. Glagola, D.J. Henderson, D.G. Kovar, C.F. Maguire, J.F. Mateja, R.G. Ohl, F.W. Prosser, J.H. Rollinson, and R.S. Trotter, Phys. Rev. C **49**, 948 (1994).
[13] R. Barná, D. De Pasquale, A. Italiano, A. Trifiró, M. Trimarchi, A. Strazzeri, V. Rauch, D. Disdier, C. Beck, T. Bellot, R.M. Freeman, R. Nouicer, M. Rousseau, and O. Stezowski, Phys. Rev. C **64**, 054601 (2001).
[14] A. Strazzeri, Nuovo Cimento A **52**, 323 (1979).
[15] A. Strazzeri, Nuovo Cimento A **71**, 1 (1982).
[16] A. Strazzeri, Nuovo Cimento A **80**, 35 (1984).
[17] A. Strazzeri, Nuovo Cimento A **81**, 595 (1984).
[18] G. Pisent and A. Strazzeri, Nuovo Cimento A **104**, 1007 (1991).
[19] A. Italiano, A. Trifiró, G. Pisent, and A. Strazzeri, Nuovo Cimento A **110**, 781 (1997).
[20] G. Bélier, Ph.D. thesis, Strasbourg University, 1994.
[21] T. Bellot, Ph.D. thesis, Strasbourg University, 1997.
[22] M. Rousseau, Ph.D. thesis, Strasbourg University, 2001.
[23] R. Barná, D. De Pasquale, A. Italiano, A. Trifiró, M. Trimarchi, V. Rauch, C. Beck, F. Haas, M. Rousseau, O. Stezowski, and A. Strazzeri, Heavy Ion Phys. **16/1-4**, 281 (2002).
[24] See EPAPS Document No. E-PRVCAN-66-026211 for color figures. This document may be retrieved via the EPAPS homepage (http://www.aip.org/pubserv/epaps.html) or from ftp.aip.org in the directory /epaps/. See the EPAPS homepage for more information.
[25] C. Bhattacharya, M. Rousseau, C. Beck, V. Rauch, R.M. Freeman, D. Mahboub, R. Nouicer, P. Papka, O. Stezowski, A. Hachem, E. Martin, A.K. Dummer, S.J. Sanders, and A. Szanto De Toledo, Phys. Rev. C **65**, 014611 (2002).
[26] M. Rousseau, C. Beck, C. Bhattacharya, V. Rauch, O. Dorvaux, K. Eddahbi, C. Enaux, R. M. Freeman, F. Haas, D. Mahboub, R. Nouicer, P. Papka, O. Stezowski, S. Szilner, A. Hachem, E. Martin, S. J. Sanders, A. K. Dummer, and A. Szanto De Toledo, Phys. Rev. C **66**, 034612 (2002).
[27] A. Trifiró, Ph.D. thesis, Messina University, 1999.
[28] M. Trimarchi, Ph.D. thesis, Messina University, 2000.
[29] H. Feshbach, C.E. Porter, and V.F. Weisskopf, Phys. Rev. **96**, 448 (1954).
[30] M.A. Preston, *Physics of the Nucleus* (Addison-Wesley, Reading, MA, 1963).
[31] W. Hauser and H. Feshbach, Phys. Rev. **87**, 366 (1952).
[32] F.L. Friedman and V.F. Weisskopf, *Niels Bohr and the Development of Physics* (McGraw-Hill, London, 1955).
[33] H. Eichner, H. Stehle, and P. Heiss, Nucl. Phys. **A205**, 249 (1973).
[34] T. Ericson and V. Strutinsky, Nucl. Phys. **8**, 284 (1958); **9**, 689 (1958).
[35] M. Lefort, in *Proceedings of the International School of Physics "Erico Fermi,"* Course LXII, Varenna, edited by H. Faraggi and R.A. Ricci (North-Holland, Amsterdam, 1976).
[36] N.K. Glendenning, International Conference on Reactions between Complex Nuclei, Nashville, 1974 (unpublished), Vol. 2 p. 137.
[37] V.M. Strutinsky, Sov. Phys. JETP **19**, 1401 (1964).
[38] J. Wilczynski, Phys. Lett. **47B**, 484 (1973).
[39] P.D. Bond, Phys. Rev. C **22**, 1539 (1980); Phys. Rev. Lett. **40**, 501 (1978).